**Research Article**

# H∞ artificial bee colony law strategy of six degrees of freedom Boeing 747-100 control augmentation

## Ezzeddin M. Elarbi[1*] and Abdulhamid A. Ghmmam[2]

Associate Professor of system modelling and simulation, The University of Tripoli, Aeronautical Engineering Department, Tripoli-Libya[1]
Professor of flight mechanics, The University of Tripoli, Aeronautical Engineering Department, Tripoli-Libya[2]

### Abstract
*The paper implements the synthesis of H-infinity ($H_\infty$) and artificial bee colony (ABC) algorithms to simulate the quasilinear six degrees of freedom (6DOF) model of Boeing® 747-100 (B747-100) flight at the baseline trim condition of Mach number and altitude of 0.5 and 6096 m respectively. Such a model has been decomposed into longitudinal and lateral motions. The main aim has been to assess such modern control approach to this ancient 1969 model plane. As the longitudinal states couple with elevator and throttle control inputs and the lateral state coupling with aileron and rudder ones, the ABC algorithm has been approved to realize the $H_\infty$ stability augmentation design ($H_\infty SAD$) for a somewhat large-scale model. The well-known $H_\infty$ weighting matrices in terms of the full state feedback gain and controlled state matrices are competently augmented for a quadratic performance on the order of nine. Overall, successful modelling simulations have been attained and converged responses are obtained in a few seconds, with negligible overshoots and steady-state errors. Stable dynamic flight spectra of various identified eigenvalues fulfil the most flying quality assets. Particularly, the short period mode has shown close agreement with the satisfactory region of the flying quality properties compared without control and linear-quadratic optimal full state feedback control conducted in the past work. The synthesis of $H_\infty$ and ABC algorithms has been verified to be a well-trusted platform for the stability augmentation design of planes.*

### Keywords
*6DOF longitudinal-lateral controls, B747-100 model, Coupling states, $H_\infty$ artificial bee colony synthesis, Flying qualities, Flight modes, Stability augmentation.*

## 1.Introduction
A degree of complexity is raised with aircraft motion as affected by axial, directional and upright forces, pitch, yaw, and roll moments and structural coupled elastic motions. The assumptions of the rigid-body aeroplane and the small deviation from trimmed flight conditions are widely considered. Thus, aircraft longitudinal and lateral equations of motion can be treated separately. In the early days of aviation, a significant pilot workload was required to ensure safe flight and passengers' comfort. Nowadays, stability augmentation systems provide satisfactory damping characteristics and stability margins and perform inner loop feedback control. Since the pioneer Sperry autopilot, such contemporary design has become vital to the airline industry to hold an attitude using several high-speed processors [1].

They are also useful in extremely long endurances to avoid pilot fatigue.

The classical control approach was widely designed for ancient autopilot models [2, 3]. However, they provide the limited robustness capability of disturbance rejections. Modern control techniques are also popular in autopilot applications of these days' computerized planes [4]. Robust control theory has been developed since 1980 to include an uncertainty between the actual plant and its model. The H-infinity ($H_\infty$) approach can superbly tackle both robustness and tracking requirements in the case of noise, disturbances and/or uncertainties. The $H_\infty$ technique is renowned for active research for an efficient, robust design practice for two decades [5].

Evolutionary and swarm intelligent optimization have been extensively used in recent years [6]. The

---

artificial bee colony (ABC) algorithm is one of the intelligent swarm techniques used for global optimization problems and evolutionary approaches. Such an algorithm shows strong survey capability despite the fact of poor manipulation performance [7]. The improved ABC was revealed by introducing a self-adaptive mechanism to enhance the performance capability [6].

As may be observed in the literature review section that many researchers have successfully used the $H_\infty$ method for particular applications while the bee colony algorithm is being applied to others of interest. However, no observations have been seen in merging both techniques in one framework to grip one large scale problem in terms of control augmentations and parameter optimisation ways. As the aim of this article is to simulate the six degrees of freedom (6DOF) flight of the Boing 747-100 (B747-100) aircraft and the increase of coupling state variables of longitudinal and lateral motions, the combined $H_\infty$ and bee colony algorithms are approved to realistically accomplish model simulation strategy and analysis appropriately.

Thus, this paper aims to simulate the 6DOF quasilinear model of the B747-100 flight at Mach number (M) of 0.5 and altitude (h) of 6096 m. The reason behind using the B747-100 refers to that most databases are open sources, e.g. the stability and control derivatives used to build and test the model are available in [1, 8] and many others. The B747-100 widely deploys that baseline flight regime to perform both longitudinal and lateral manoeuvring motions. The multivariable nature underlying aircraft motion is represented by a quasilinear state-space model. The quasilinear model uses the decomposition of the longitudinal state variables coupling with elevator and throttle actuators and the lateral-directional state variables with aileron and rudder actuators. Such a large-scale model comprises a system, control weighting matrices and their parameters to be optimised. The combination of $H_\infty$ and ABC methods is used to augment the degree of freedom for a quadratic performance of such a flight scenario and ease design parameter optimization of the large-scale coupling variables. This platform is named the $H_\infty$ stability augmentation design ($H_\infty$SAD) approach. The SeDuMi MATLAB® package [9] is used to implement the $H_\infty$SAD for 6DOF B747-100 flight simulation and control.

State flight variables are converged within a few seconds showing negligible overshoot and transient behaviour. Finally, the fine-tuning responses have been attained based on the reference input full-state feedback autopilot [10]. Those responses meet the objectives of flight speed of 157.9 m/sec and altitude of 6096 m. The derived model is verified based on whether the response of the controlled plane obeys flying qualities' requirements for longitudinal and lateral modes. However, the general pilot inputs and mission tasks are widely investigated by the flying qualities and/or handling qualities [8]. Acceptable stable eigenvalues are found satisfying B747-100 flying qualities' primarily requirements of the longitudinal modes (short period and phugoid long period) and the lateral modes (roll subsidence, spiral convergence and Dutch roll). Feasibly acceptable agreements are seen to short-period, control anticipation parameter (CAP) and pitch rate flying qualities based on various flight conditions in comparison with the linear quadratic regulator (LQR) [10] and the standard constraints [1, 8].

The paper is organised into five sections in addition to the present introduction section. Section 2 reviews available literature on similar work research. Section 3 shows the analysis approach in the form of the 6DOF flight model, flight modes, $H_\infty$ control algorithm and ABC method. Section 4 shows the results obtained in terms of 6DOF flight characteristics, 6DOF flight responses, 6DOF flight control effort and 6DOF flight control validations. Section 5 gives the discussion in the form of a comparative analysis of the obtained simulation and the limitations associated with it. Section 6 gives the conclusions and future work.

## 2.Literature review
The comprehensive, literate review has been conducted to highlight feasibly similar applications proposed as well as implemented during the timeframes of ongoing research. It was so hard to find research using a combined $H_\infty$ control and ABC optimisation algorithm in one framework to model the 6DOF B747 flight. Many articles as shown below used $H_\infty$ control to obtain robust performance and track operating status for miscellaneous applications ranging from unmanned vehicles to space shuttles. Similarly, the ABC algorithm is widely proven as a powerful global optimisation strategy for so many large-scale problems. However, the 6DOF flight of motion of widespread applications was widely approached using the LQR.

Tosun et al. [11] used LQR control for the Quadrotor X4 (Qball-X4) which includes positions, roll, pitch

and yaw models, and the position control reaches desired attitudes. An integral-LQR-based was incorporated in 6DOF control of a small-scale quadcopter to provide high dynamic control tracking and balancing system responses [12]. The LQR control stabilised the attitude and altitude of the star-shaped Octrotor vehicle showing its effectiveness under nominal conditions [13]. An LQR controller was successfully implemented in the real-time pitch axis helicopter stabilisation for reference tracking as high as 55 degrees [14]. Satisfactory performance was also found during all the yaw angles for a Quadrotor Sabanci University Unmanned Aerial Vehicle (QSUAVE) which has a skewed wing structure system [15].

Sharma et al. [16] deployed autopilot pitch attitude control for an icing condition. H-Two (H2) control provides an optimisation means of systematic design of high-order systems. Lungu and Lungu [17] presented the H∞ control approach of the Boeing 747 (B747) landing longitudinal plane using optimal observer (OO). The simulation results are as respectable as the theoretical results in terms of the altitude, the landing curve velocity, and the associated derivatives of the system. Federal Aviation Administration (FAA) accuracy requirements for category III (CIII) are met demonstrating the robustness of the algorithm in the presence of wind shears and sensor errors. Portapas and Cooke [18] studied the full model of rigid and morphing wing aircraft flying qualities criteria. They found an insignificant difference in the longitudinal ad lateral/directional model in those criteria between rigid wing aircraft. However, their real-time tests showed the degraded discrepancies of those criteria on both the longitudinal and lateral/directional flights.

Rigatos and Siano [19] introduced a recursive H∞ control solution for the mobile robot system. Local linearization of the vehicle system model was made at the existing position using Jacobian matrices feedback control law (JM-FCL) to figure out the stability requirements. The robot tracked all reference paths and executed parallel parking. Zhang et al. [20] discussed an event-triggered load frequency network power control problem. The stabilization criteria were reached using the Lyapunov and linear inequality matrix methods. Computational illustrations reveal the effectiveness of the results. The adaptive threshold event-triggered new scheme exceeds the performance of a fixed old threshold. Luo et al. [21] used the inverse optimal H∞ approach

to address the attitude control of trajectory rigid spacecraft in the presence of abrupt environments. The computational tuning guidelines (CTG) were practised showing the usefulness of the offered control algorithm.

A distributed $H_\infty$ control technique was presented for identical dynamic and rigid geometry of grouped autos [22]. The information exchange topology matrix (IETM) of the platoon control system was fragmented into two sections: uncertain and diagonal nominal. Robust stability, string stability and distance tracking performance were analysed theoretically based on the decoupled $H_\infty$ framework. The effectiveness was shown by a comparative simulation with no robust controllers. The attitude and position control were used to investigate the track performance to unknown multiplicative actuator faults of the lead-wing system [23]. In the case of a lead wing unmanned plane in maneuverer, an adaptive fault-tolerant $H_\infty$ feedback output control (FOC) was considered for the asymptotic stability performance and tracking merits. The efficiency of the proposed fault-tolerant control algorithm was validated by simulation results.

A back-stepping $H_\infty$ control approach for the uninhabited plane was proposed with time-depended disturbances [24]. Lyapunov functions (LF) were used to probe the attitude and position of the vehicle. The recursive $H_\infty$ back-stepping proposal was applied for disturbance rejection based on the virtual inputs. The positions and attitude system response were verified by two reference variables. A new H∞ output dynamic feedback synthesis is offered based on linear matrix inequality and equality parameterizing [5]. The main design parameters in the optimal control algorithm such as LQR and H∞ are the selection of weighting matrices. However, traditional approaches are time-consuming and require highly experienced applicants to achieve a robust design in both the time and frequency domains. In this connection, genetic and particle swarm algorithms have been recently proposed in many artificial intelligent optimization procedures [25]. On the other hand, the dynamic inversion part of the H∞ method provides good precision tracking. Thus, the developed H∞ may guarantee asymptotic stability, system performance, and tracking properties in comparison with LQR [22].

The ABC procedure is widely approached for optimizing parameter weighting matrices. The ABC set of rules comes under the swarm intelligent

optimizer category which is knowingly useful for multivariable functions. The ABC intelligently behaving method of honey bee swarms algorithm was firstly introduced by Karaboga in 2005 to optimize numeric benchmark functions [25]. Baris and Coban [26] used combined ABC with LQR optimal control for a nonlinear inverted pendulum. It was found from the simulations that the outstanding efficiency of the ABC procedure in optimizing weighting matrices compared to the traditional tedious trying-based methods such as trial and error Thumps' rules (TETR).

Karaboga and Akay [27] extended the past work [25] to overcome the drawbacks of heuristic methods like particle swarm optimization, genetic algorithm and differential evolution algorithm. The extended ABC procedure becomes stronger robustly, fast converged and highly flexible. Multidimensional and multimodal optimizations can be solved by reduced control parameters [27]. A self-adaptive ABC method was suggested using the finest candidate of overall optimization [6]. 25 benchmark functions were examined in an actual cluster with the K-means method. The fresh optimization algorithm was greater than the others in handling complex problems. The performances of employed and onlooker bees are more pronounced after introducing the new ABC updating equations [7]. New bee control operators in the intelligent learning schemes can easily perform better in learning from individuals and in balancing global and local searches. A new exploration strategy overcame the oscillatory behaviour of active bees. The proposed intelligent learning strategy caused the worst active bee to hook reasonable convergence.

The control system designer toolkit was used to investigate a nonlinear B747-100 trimmed model [28]. A state-feedback controller was tested for a computerised aircraft integrated synthesis (CAIS) optimiser to adjust the longitudinal flight. A defective aerodynamic surface and imperfect engines were extensively explored by the closed-loop designs. A fully nonlinear B747-100 was easily analysed by highly featured adaptive-fidelity aerodynamic data deployed by the linear control method [28]. The fault-tolerant control scheme was successfully implemented for the nonlinear benchmarks of Boing 747-100/200 (B747-100/B747-200) to safely land aircraft when elevators were stuck as major actuator faults by reducing optimized parameters [29]. Laguerre functions model predictive control scheme (LFMPC) improved online capability where the time delay was integrated into the feedback control loop to

redistribute the control efforts to the remaining actuators [29].

Hameed and Bindu [30] integrated an LQR with the gain scheduling (GS) control scheme for the touchdown vehicle's merits of approach and landing phases. The application was adequately robust to tackle drag problems during these stages under off-nominal initial conditions. Eser and Cetin [31] used the ABC optimisation method to augment torque control of flexible manipulators in every sampling epoch. They achieved promising position control with suppressed vibration for various payloads by optimizing three parameters in torque control. Ma et al. [32] deployed the ABC procedure to obtain the optimal design matrices of the LQG-based loop transfer recovery algorithm applied for trajectory tracking and attitude control of a small-scale unmanned helicopter. Flight tests are well compared with simulations based on the effectiveness and robustness of such a two-loop hierarchical control design. Saied et al. [33] demonstrated by Matlab/Simulink simulations how the ABC is being individually used for several unmanned aerial vehicles. The arrangement satisfactorily helped in avoiding obstacles and collisions by finding velocity controls of the fleet and tracking system.

Du et al. [34] suggested the ABC optimize parameters of the proportional-integral-derivative (PID) compensator for a global solution based on the improved source probability. It is stated that the PID with reformative ABC (RABC) had better performance in terms of lowest overshoot and swift response in comparison with other PID arrangements for various tested systems. Cai and Liu [35] investigated the 6DOF flight control using the proportional-derivative (PD) scheme optimized by Laplace transformation and root locus (LT-RL) method for flapping-wing unmanned planes application based on bioinspired bumblebee hovering flight. Their strategy stabilized the vertical position with yawing, pitching and rolling kinematics while the forward/backward position and lateral position stabilized with the decoupling kinematics of pitching and rolling. Du et al. [36] also optimised a PID control radar-servo system by RABC strategy. It was shown by the simulation that particle swarm optimization, differential evolution, and genetic algorithm could not do better than their proposed scheme in controlling the system. Sheida et al. [37] showed another successful implementation of the PID and ABC algorithms for depth control of an autonomous submarine tanker by effectively reducing

the steady-state and the overshoot more than without incorporating the ABC. Jouda and Kahraman [38] found that H∞ control performance can be enhanced with the ABC set of rules for stable electric grid applications. Superb performances are achieved over traditional droop control, and particle swarm optimization algorithms in reducing the overshoot, boosting the robustness against external disturbance.

Since the paper scope is not reviewing research, the authors have attempted to document most research articles that either use methods similar to the main applications here or are relevant to the subject of this paper. However, a variety of research papers based on the usage of the ABC optimiser in widespread engineering applications may be found in [39−44] for the wider interest of readers. Overall, the review analysis is conducted based on the represented literature above. *Table 1* shows a summary of the key papers by comparing the method, optimiser algorithm, application, result and limitation. The ABC algorithm outperforms swarm optimization,

differential evolution, and genetic algorithm in the effectiveness optimisation techniques for executing weighting matrices used in optimal control theory. However, no broad applications have been noticed using the synthesis of the $H_\infty$ and ABC approach apart from recently being used for the electric network [38]. Even such that application does not represent a highly dynamic system like the 6DOF aircraft flight model which is supposed highly coupled states of a nonlinearity nature. Therefore, this paper will be novel research exploiting the most robust, fast convergence and highly flexible feature of the ABC algorithm into multidimensional and multimodal optimizations of $H_\infty$ control parameters for the 6DOF B747-100 flight model. Thus, the authors avoided using a classical time-consuming approach to achieve a robust design. Most comparable focuses are noticed in references [12, 17, 35] where integral LQR based on TAETR optimiser, H∞ with OO optimiser and PD with LT-RL optimiser are used respectively.

**Table 1** Overall review analysis of literature

| METHOD | OPTIMIS | APPLICATION | RESULT | LIMITATION | REF. |
|---|---|---|---|---|---|
| LQR | TAETR | Qball-X4 | reasonable attitudes | low degree model | [11] |
| Integral LQR | TAETR | 6DOF quadcopter | tracking and balancing responses | small-scale control problem | [12] |
| LQR | TAETR | Octrotor vehicle | attitude stabilisation | under nominal conditions | [13] |
| LQR | TAETR | helicopter | real-time pitch stabilisation | pitching reference | [14] |
| LQR | TAETR | QSUAVE | satisfactory performance | yaw angle model | [15] |
| $H_\infty$ | OO | B747 landing system | robust CIII FAA criteria | low-intensity sensor errors | [17] |
| Recursive $H_\infty$ | JM-FCL | mobile robot | track reference paths | local position linearisation | [19] |
| Inverse $H_\infty$ | CTG | spacecraft | addressed attitude trajectory | under abrupt environment | [21] |
| Distributed $H_\infty$ | IETM | grouped autos | More effective than no robust controllers | decoupled framework | [22] |
| Adaptive $H_\infty$ | FOC | lead-wing unmanned plane | efficiency validated simulation results | asymptotic stability performance | [23] |
| Recursive $H_\infty$ | LF | uninhabited plane | verified positions and attitude response | virtual inputs | [24] |
| State feedback | CAIS | B747-100 trimmed model | adjustable longitudinal flight | linearised aerodynamic data | [28] |
| Fault-tolerant | LFMPC | B747-100/B747-200 landing aircraft | successfully nonlinear benchmarks | reduced and optimized parameters | [29] |
| LQR | GS | approach and landing touchdown vehicle | robust tackling drag problems | under off-nominal initial conditions | [30] |
| PID | ABC | global problem solution | lowest overshoot and swift response | artificial source probability | [34] |
| PD | LT-RL | 6DOF flapping wing micro aerial vehicles | satisfactorily stabilized flight positions | bioinspired hovering bumblebee kinematics | [35] |
| PID | RABC | radar-servo system | higher performances than other optimisations | moderately scaled weighting matrices | [36] |
| $H_\infty$ | ABC | electric network | superb performances | unverified disturbances | [38] |

# 3. Methods (Analysis approach)

## 3.1 6DOF flight model

The full dynamic derivations of aircraft motion can be found in [1, 8]. The 6DOF flight model represents longitudinal and lateral motions that combine three linear translations, rolling, pitching, yawing and side-slipping motions. Using a small perturbation assumption the longitudinal and lateral motions can be simulated based on a quasilinear model which should be quite equivalent to the full 6DOF of a flight model. The dynamic system which represents the state and response equations is expressed as in Equation 1.

$$\begin{bmatrix} \dot{X} \\ y \end{bmatrix} = \begin{bmatrix} A & B \\ C & D \end{bmatrix} \begin{bmatrix} x \\ \Delta\delta \end{bmatrix} : X = \dot{x} \qquad (1)$$

where the system matrix (A), control matrix (B), observation matrix (C), and transition matrix (D).

Thus, Equation 1 can be reformulated for the 6DOF quasi-linearized flight model as below (Equation 2).

$$\begin{bmatrix} \Delta\dot{u} \\ \Delta\dot{v} \\ \Delta\dot{w} \\ \Delta\dot{p} \\ \Delta\dot{q} \\ \Delta\dot{r} \\ \Delta\dot{\Phi} \\ \Delta\dot{\theta} \\ \Delta\dot{h} \end{bmatrix} = \begin{bmatrix} X_u & 0 & X_w & 0 & 0 & 0 & 0 & -g & 0 \\ 0 & Y_v & 0 & Y_p & 0 & Y_r & g & 0 & 0 \\ Z_u & 0 & Z_w & u_0 & 0 & 0 & 0 & 0 & 0 \\ 0 & L_v & 0 & L_p & 0 & L_r & 0 & 0 & 0 \\ M_u & 0 & M_w & 0 & M_q & 0 & 0 & 0 & 0 \\ 0 & N_v & 0 & N_p & 0 & N_r & 0 & 0 & 0 \\ 0 & 0 & 0 & 1 & 0 & 0 & 0 & 0 & 0 \\ 0 & 0 & 0 & 0 & 1 & 0 & 0 & 0 & 0 \\ 0 & 0 & -1 & 0 & u_0 & 0 & 0 & 0 & 0 \end{bmatrix} \begin{bmatrix} \Delta u \\ \Delta v \\ \Delta w \\ \Delta p \\ \Delta q \\ \Delta r \\ \Delta\Phi \\ \Delta\theta \\ \Delta h \end{bmatrix}$$

$$+ \begin{bmatrix} X_{\delta_e} & 0 & X_{\delta_t} & 0 \\ 0 & Y_{\delta_a} & 0 & Y_{\delta_r} \\ Z_{\delta_e} & 0 & Z_{\delta_t} & 0 \\ 0 & L_{\delta_a} & 0 & L_{\delta_r} \\ M_{\delta_e} & 0 & M_{\delta_t} & 0 \\ 0 & N_{\delta_a} & 0 & N_{\delta_r} \\ 0 & 0 & 0 & 0 \\ 0 & 0 & 0 & 0 \\ 0 & 0 & 0 & 0 \end{bmatrix} \begin{bmatrix} \Delta\delta_e \\ \Delta\delta_a \\ \Delta\delta_t \\ \Delta\delta_r \end{bmatrix}$$

(2)

where a steady-state velocity ($u_0$) and a gravity acceleration ($g$) of 9.81 m/sec. Forward velocity ($u$), side velocity ($v$), and upright velocity ($w$). The roll rate ($p$), pitch rate ($q$), and yaw rate ($r$). Pitch angle ($\theta$) and bankroll angle ($\Phi$). Elevator control ($\delta_e$), throttle control ($\delta_t$), aileron control ($\delta_a$), and rudder control ($\delta_r$). Derivatives are forwarding forces concerning forwarding velocity ($X_u$) and concerning normal velocity ($X_w$). Those are of normal forces concerning side velocity ($Y_v$), concerning roll rate ($Y_p$), and concerning yaw rate ($Y_r$). Those are side forces concerning forwarding velocity ($Z_u$), and concerning normal velocity and ($Z_w$). Derivatives are of roll moment with respect to side velocity ($L_v$), concerning roll rate ($L_p$), and with respect to yaw rate

($L_r$). Those are of yaw moment with respect to side velocity ($N_v$), with respect to roll rate ($N_p$), and with respect to yaw rate ($N_r$). Those are of pitch moment with respect to forwarding velocity ($M_u$), normal velocity ($M_w$), and with respect to pitch rate ($M_q$). The angle of attack ($\alpha$) and the sideslip angle ($\beta$) are approximately obtained using $\Delta\dot{\alpha}(\Delta\dot{\beta}) = \Delta\dot{w}(\Delta\dot{v})/V$. The aircraft velocity ($V$) of 157.9 m/sec at M = 0.5. The first and second matrices of Equation 2 in turn represent A ($9 \times 9$ aircraft matrix) and B ($9 \times 4$ control matrix). Since the states were taken as system outputs ($y = x$), the C and D would be taken $9 \times 9$ unity and $9 \times 4$ nullity matrices respectively. The flight states are $x =$ $[\Delta u \quad \Delta v \quad \Delta w \quad \Delta p \quad \Delta q \quad \Delta r \quad \Delta\Phi \quad \Delta\theta \quad \Delta h]^T \in R^9$ and the control actions are $\Delta\delta = [\Delta\delta_e \quad \Delta\delta_a \quad \Delta\delta_t \quad \Delta\delta_r]^T \in R^4$.

## 3.2 6DOF flight modes

The longitudinal motion transfer functions of forwarding velocity, normal velocity, pitch rate, pitch angle and altitude with respect to the elevator and/or throttle controls are derived as shown in below Equation 3,

$$\frac{u \mid w \mid q \mid \theta \mid h}{\Delta\delta_e \mid \Delta\delta_t} \left( \frac{v \mid p \mid r \mid \emptyset \mid \beta}{\Delta\delta_a \mid \Delta\delta_r} \right) = \frac{a_4 s^4 + a_3 s^3 + a_2 s^2 + a_1 s + a_0}{b_5 s^5 + b_4 s^4 + b_3 s^3 + b_2 s^2 + b_1 s + b_0}$$

(3)

where those transfer functions have different numerator coefficients ($a$s) and different denominator coefficients ($b$s). $a_i : i = 0, 1, \dots, 4$ are the numerator coefficients of absolute term, $s$ term, …, forth power of $s$ Laplace variable. $b_i : i = 0, 1, \dots, 5$ are the denominator coefficients of absolute term, $s$ term, …, fifth power of $s$ Laplace variable. Similarly, the lateral motion transfer functions of side velocity, roll rate, yaw rate, bank and sideslip angles concerning aileron and/or rudder controls are also shown by Equation 3 in the brackets. Equation 3 could be easily obtained by manipulating $C_l(sI - A)^{-1}B$ whose $C_l$ is the $l^{th}$ row of $C$ corresponding to those transfer functions needed to be found ($l = 1, 2, \dots, 5$). The resultant responses are then found by combining the transfer functions of the elevator and throttle for longitudinal flight actuation and by combining the transfer functions of the aileron and rudder for lateral flight actuation. The polynomial characteristic equation of longitudinal motion, which is the denominator of Equation 4, can usually be factorized into the following

$$b_5 s^5 + b_4 s^4 + b_3 s^3 + b_2 s^2 + b_1 s + b_0$$
$$= \lambda(\lambda^2 + 2\xi\omega\lambda + \omega^2)_{PH} (\lambda^2 + 2\xi\omega\lambda + \omega^2)_{SP}$$

(4)

a. Phugoid (PH) or long period mode is represented by the quadratic term $(\lambda^2 + 2\xi\omega\lambda + \omega^2)_{PH}$ which has a small damping ratio and slow aircraft motion with large oscillatory changes in $u$, $h$, and $\theta$.

b. Short Period (SP) mode is represented by the quadratic term $(\lambda^2 + 2\xi\omega\lambda + \omega^2)_{SP}$ which has a large damping ratio and quick aircraft motion with small oscillatory changes in $\alpha$ or $w$ and $q$.

Also, the polynomial characteristic equation of lateral motion, which is also the denominator of Equation 3, can usually be factorized into the following (Equation 5).

$$b_5 s^5 + b_4 s^4 + b_3 s^3 + b_2 s^2 + b_1 s + b_0$$
$$= \lambda(\lambda + e)(\lambda$$
$$+ f)(\lambda^2 + 2\xi\omega\lambda + \omega^2)_{DR}$$
$$(5)$$

a. Spiral Convergence mode (SC) is represented by the term $(\lambda + e)$ which has a very slow motion of a long-term tendency either to maintain the wings level or to 'roll off' in a divergent spiral.

b. Rolling Subsidence mode (RS) is represented by the term $(\lambda + f)$ which is fairly faster than the SC mode.

c. Dutch Roll oscillatory mode (DR) is represented by the quadratic term $(\lambda^2 + 2\xi\omega\lambda + \omega^2)_{DR}$ which has a small damping ratio.

where the damping ratio $(\xi)$ and undamped natural frequency $(\omega)$. The aircraft Eigenvalue $(\lambda)$ will justify those modes above illustrated based on Equation 4 and Equation 5. Besides, once an aircraft's heading has been changed there is no natural tendency to be restored to its equilibrium heading. Such a scenario represents the simple directional mode at $\lambda = 0$. An aircraft has neutral heading stability using some corrective control action to bypass the issue of perturbed heading.

### 3.3 H$_\infty$ control algorithm

The H$_\infty$ sufficient condition is given under linear matrix inequality and linear matrix equality constructions of an output control robust system. H∞ defines the whole stable linear domains in which the extreme energy gain is determined. Also, the maximum singular frequency response matrix is defined over the entire frequencies [5]. A full order time-invariant dynamic output controller is (Equation 6 and 7).

$$\dot{q} = Jq + Lx \tag{6}$$
$$\Delta\delta(t) = Mq + Nx \tag{7}$$

$q = [q_1 \quad q_2 \quad q_3 \quad \cdots \quad q_i]^T \in R^9$ is the vector of controller state variables. Since aircraft control

722

systems may be considered strictly proper as no evident link between the command actuators and the measuring variables, *i.e.*, D = 0. The weighting structure matrix is shown below (Equation 8).

$$K^\circ = \begin{bmatrix} J & L \\ M & N \end{bmatrix} \tag{8}$$

where $K^\circ \in R^{13\times18}$ has the prescribed dynamic concerning the real matrices $J \in R^{9\times9}$, $L \in R^{9\times9}$, $M \in R^{4\times9}$ and $N \in R^{4\times9}$ to be designed. The objective is to design the control law matrix parameters not exceeding a specified limit defined as the guaranteed quadratic performance. The closed-loop transfer function matrix is then optimised based on the H$_\infty$ norm asset. By only considering the control, the measured variable output vector *y(t)* was formulated by the H$_\infty$ norm square of the closed-loop transfer function matrix. Thus, it has to reduce the control energy $(\sigma\sim1)$. $K \in R^{4\times9}$ is an unknown gain matrix (Equation 9 and 10).

$$\|K(I + GK)^{-1}\|_\infty < \sigma \tag{9}$$

$$G(s) = \begin{bmatrix} A & B \\ C & 0 \end{bmatrix} \tag{10}$$

Using the Schur's complement property then the inequality matrix implies [5].

$$\begin{bmatrix} AQ + QA^T + BYC + C^TY^TB^T & 0 & CQ \\ 0 & -\gamma I_p & 0 \\ CQ & 0 & -I_n \end{bmatrix} < 0 \tag{11}$$

where $Q = Q^T > 0$, $I_p$ and $I_n$ indicate the p$^{th}$ and n$^{th}$ order unit matrices and $\gamma > 0$.

Analysing the inequality components of Equation 11 when CQ = HC, the below condition has to be obeyed as shown in Equation 12.

$$BKCQ = BKHH^{-1}CQ \tag{12}$$

The valid condition above derives the gain matrices of the output control rule set by the formula (Equation 13).

$$K = YH^{-1} \tag{13}$$

Thus, the close loop control matrix $A_C$ is noted as (Equation 14).

$$A_C = (A + BKC) \tag{14}$$

The static output controller has stable quadratic performance for a positive scalar $\gamma \in R$ and a positive definite symmetric matrix $Q \in R^{9\times9}$, a regular matrix $H \in R^{9\times9}$ and matrix $Y \in R^{4\times9}$. The output-controlled variables are expressed by the following scheme (Equation 15).

$$\Delta\delta(t) = -Kx(t) + Ww(t) \tag{15}$$

where $w(t) \in R^9$ is the preferred output vector and $W \in R^{4 \times 9}$ is the gain matrix. Thus, the closed-loop gain matrix inversion results in the matrix W which merely represents the static decoupling norm (Equation 16).

$$W = -\left(CA_C^{-1}B\right)^{-1} \qquad (16)$$

The exceeding arrangement can practically track the command singles, i.e., $y(t)$ tracks $w(t)$, particularly in the case of slowly enough variations [5].

## 3.4ABC algorithm

The ABC technique is a well-known systematic procedure that is widely used to optimise the weighting matrices as many applications of swarm intelligent optimization appreciatively do. Generally, the ABC phases cover initialization, employed bees, onlooker bee and scout bees phases. The full pseudo-ABC algorithm is as below summarised [26],

1. Resetting and evaluating the attained inhabitants
2. Iterating cycle one
3. Producing and evaluating new solutions $\Lambda_{ij}$ around the employed bees (Equation 17)

$$\Omega_{ij} \, \Lambda_{ij} = \Omega_{ij} + \mu_{ij}(\Omega_{ij} - \Omega_{kj}) \qquad (17)$$

$k$ is an evaluation at the $i$ vicinity and $\mu$ is an arbitrary array around minus-plus one.

4. Prompting the greedy range course between $\Omega_i$ and $\Lambda_i$.
5. Computing the suitability evaluation of the likelihood $P_i$ based on $N$ number of possible solutions (Equation 18).

$$P_i = 1/(1+f)/(\sum_{i=1}^{N} 1/(1+f_i)): f_i \geq 0 \quad (18)$$

6. Constructing unique objective function $f_i$ from some objective functions due to multi-objective optimization [26] (Equation 19).

$$f_i = \sum_{i=1}^{n} F_i \, O_i \qquad (19)$$

$O_i$ is the design objective setting including desired overshoot, settling and steady-state errors and $F_i$ is control residual parameter.

7. Normalising $P_i$ for the range from zero to one.
8. Producing and evaluating the fresh onlookers' spot $\Lambda_i$ from the evaluations $\Omega_i$ and $P_i$ normalisation.
9. Re-prompting the greedy course between $\Omega_i$ and $\Lambda_i$ for the onlookers.
10. Replacing the accessible abandoned evaluation with freshly formed ones $\Omega_i$ for the lookout horizon (Equation 20).

$$\Omega_{ij} = min \, \Omega_j + rand(0,1)(max \, \Omega_j - min \, \Omega_j) \qquad (20)$$

11. Spotting the finest evaluation realized to this point.
12. Cycling and updating to the next iteration.
13. Terminating the execution for the total cycles reached.

## 3.5Methodology diagram

*Figure 1* demonstrates the methodology for the 6DOF B747-100 flight controlled by H$_\infty$SAD and ABC algorithms. The procedure starts by papering the data of the flight model and small perturbation assumptions are made including setting ($y = x$), $C =$ unity matrix and $D =$ nullity matrix, and quasilinear 6DOF model (Equation 2). Such a model has to be decomposed into longitudinal and lateral flight but under coupling elevator and throttle control and coupling aileron and rudder control respectively. Then the model is ready to be actuated using the unit step function at M and h with $A$ and $B$ conditions. The H$_\infty$SAD algorithm is then imposed by initialising $(Q, H, J, L, N, M)$. The H$_\infty$SAD algorithm (Equation 6 - Equation 16) is used to augment the model stability. The flight convergences are checked based on the satisfactory responses of Equation 3 – Equation 5. If the responses are not valid the ABC algorithm including (Equation 17 - Equation 20) is executed to optimise $(Q, H, J, L, N, M)$. The results are also validated with flying quality criteria based on short-period mode contours. If other M and h flight cases show inappropriate responses the ABC step is executed again for another optimisation setting. The procedure is terminated at the end of the investigation or the ABC algorithm does not perform as expected in terms of its own stability performance.
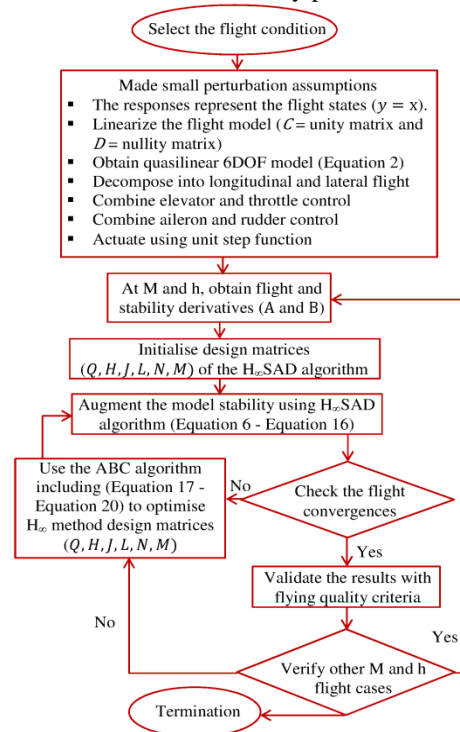


**Figure 1** Methodology flow chart for 6DOF B747-100 flight controlled by H$_\infty$SAD and ABC algorithms

# 4.Results

## 4.1 6DOF flight characteristics

The augmented matrices of Q, H, L, M, N and J that minimise $f_i$ were readily obtained by deploying the ABC procedure formerly shown. Equation 19 was applied with the optimization constraints $(O_i)$ were assumed $O_1 = 1.6\%$ overshoot and $O_2 \leq 1.5$ sec settling time which results in $f = 0.016 + 1.5 + 0.9 \times 10^{-8} = 1.516$ providing the step steady-state constrain fulfilling $O_3 = \lim_{t \to \infty} x(t) = -A^{-1}B\delta$ must die out as $t \to \infty$ for any initial perturbation to assure the dynamic stability of the aircraft system. $f_i (i = 1:3)$ are weighing quantities in the fit definitions $F_i (i = 1:3)$ and their values were chosen as 0.8, 0.75 and 0.9 respectively. All the initial employed bee matrices $\Omega_{ij}$ and $\Omega_{kj}$ have been chosen diagonally valued based on trial-and-error procedures. The ABC factors were set between 0.1 and 100, the inhabitant dimension was taken at 15 and the total cycle was not exceeded around 100. Moreover, the maximum number of generations was fixed to 1000 and $D \times N$ was considered for coefficient restrictions, where $D \in R^{13 \times 18}: R^{9 \times 9}: R^{4 \times 9}$ signifies the exploration size. The algorithm was run for 20 runtimes on each benchmark case before validating the obtained solution.

The weighting matrices (K) obtained by the ABC algorithm shown by Equation 13 which satisfies the inequality matrix condition in Equation 11 gave the gain matrix as next. Equation 2 was used to model the 6DOF B747-100 flight by filling all the aerodynamic and stability derivatives at M = 0.5 and h = 6096 m [8]. Thus, the resulting quasilinear model which was used to perform both longitudinal and lateral manoeuvring motion simulation is shown next. The controlled state matrix $(A_C)$ is now revised as shown in Equation 22 by including the influence of the full state feedback gain matrix above based on Equation 14.

The B747-100 aircraft was simulated by implementing the above gain feedback matrix obtained based on the $H_\infty$ and ABC algorithm to investigate the realisation of the 6DOF controlled flight. The plane was excited to respond to unit step-input reference states so that the foremost influence of altitude was obtained from 1° roll, pitch and yaw angles and the foremost influence of thrust was obtained from 1° throttle defection and 157.9 m/sec flight velocity. The resultant lateral-directional coupling control is executed by combined actuation of the aileron and rudder for the lateral flight motion $(\Delta\delta_{ar} = \Delta\delta_a \cup \Delta\delta_r)$ whereas the resultant longitudinal coupling control is performed by combined actuation of elevator and throttle for the longitudinal flight motion $(\Delta\delta_{et} = \Delta\delta_e \cup \Delta\delta_t)$. Thus, Equation 2 can now be updated for 6DOF flight analysis as shown in Equation 23.

$$K = \begin{bmatrix} 0.043 & 0 & -68.8 & 0 & -87.7 & 0 & 0 & -527.2 & 497.4 \\ 0 & 0.256 & 0 & -47.757 & 0 & -170955 & -138.539 & 0 & 0 \\ 0.078 & 0 & -124.5 & 0 & 53.8 & 0 & 0 & 507.6 & 867.5 \\ 0 & 1.682 & 0 & 4.791 & 0 & -49.773 & 24.963 & 0 & 0 \end{bmatrix} \quad (21)$$

$$A_C = \begin{bmatrix} -0.053 & 0 & 321.59 & 0 & 4.699 & 0 & 0 & 5.003 & -1141.41 \\ 0 & -3.562 & 0 & -9.909 & 0 & -54.952 & -41.815 & 0 & 0 \\ 0 & 0 & -110.03 & 0 & 0.653 & 0 & 0 & -6.42 & 395.76 \\ 0 & -0.225 & 0 & -7.485 & 0 & 5.722 & -21.522 & 0 & 0 \\ 0.0001 & 0 & -15.32 & 0 & -128.04 & 0 & 0 & -219.27 & 358.09 \\ 0 & 0.667 & 0 & 0.996 & 0 & -19.94 & 7.419 & 0 & 0 \\ 0 & 0 & 0 & 1 & 0 & 0 & 0 & 0 & 0 \\ 0 & 0 & 0 & 0 & 4 & 0 & 0 & 0 & 0 \\ 0 & 0 & -2 & 0 & 2.47 & 0 & 0 & 0 & 0 \end{bmatrix}$$

$$(22)$$

$$
\begin{bmatrix} \Delta\dot{u} \\ \Delta\dot{v} \\ \Delta\dot{w} \\ \Delta\dot{p} \\ \Delta\dot{q} \\ \Delta\dot{r} \\ \Delta\dot{\Phi} \\ \Delta\dot{\theta} \\ \Delta\dot{h} \end{bmatrix} =
\begin{bmatrix}
-0.003 & 0 & 0.0782 & 0 & 0 & 0 & 0 & -9.81 & 0 \\
0 & -0.08 & 0 & 0 & 0 & -157.9 & 9.81 & 0 & 0 \\
-0.068 & 0 & -0.433 & 156.06 & 0 & 0 & 0 & 0 & 0 \\
0 & -0.001 & 0 & -0.651 & 0 & 0.378 & 0 & 0 & 0 \\
0.0003 & 0 & -0.006 & 0 & -0.511 & 0 & 0 & 0 & 0 \\
0 & 0.003 & 0 & -0.068 & 0 & -0.142 & 0 & 0 & 0 \\
0 & 0 & 0 & 1 & 0 & 0 & 0 & 0 & 0 \\
0 & 0 & 0 & 0 & 1 & 0 & 0 & 0 & 0 \\
0 & 0 & -1 & 0 & 157.88 & 0 & 0 & 0 & 0
\end{bmatrix}
\begin{bmatrix} \Delta u \\ \Delta v \\ \Delta w \\ \Delta p \\ \Delta q \\ \Delta r \\ \Delta \Phi \\ \Delta \theta \\ \Delta h \end{bmatrix} +
\begin{bmatrix}
0.616 & 0 & 0.4617 & 0 \\
0 & 0 & 0 & 2.068 \\
-1.570 & 0 & -0.016 & 0 \\
0 & -0.128 & 0 & -0.017 \\
-1.090 & 0 & 0.248 & 0 \\
0 & -0.017 & 0 & -0.392 \\
0 & 0 & 0 & 0 \\
0 & 0 & 0 & 0 \\
0 & 0 & 0 & 0
\end{bmatrix}
\begin{bmatrix} \Delta\delta_e \\ \Delta\delta_a \\ \Delta\delta_t \\ \Delta\delta_r \end{bmatrix}
\tag{23}
$$

### 4.2 6DOF flight responses

The responses of the 6DOF-controlled B747-100 flight are investigated at the baseline of M = 0.5 and h = 6096 m. The $H_\infty$SAD was used to obtain converged simulations in terms of fast responses, negligible overshoots and steady-state errors. The ABC optimization delivered the full state feedback gains and controlled state matrices which were important to achieve an adequate realisation of the 6DOF-controlled B747-100 flight. Overall, the aircraft motion exhibited respectable responses with low overshoot, small settling time and negligible oscillations.

*Figure 2* shows the responses of forwarding velocity ($u/\Delta\delta_{et}$), side velocity ($v/\Delta\delta_{ar}$) and normal velocity ($w/\Delta\delta_{et}$). Smooth responses were obtained for the three components. The forward velocity response is slower than the side and normal velocities. The settling times for $u/\Delta\delta_{et}$, $v/\Delta\delta_{ar}$ and $w/\Delta\delta_{et}$ are almost 6 sec, 2 sec and 0.5 sec respectively. No obvious overshoots are seen and the forward, side and normal velocities are equal to 146.4 m/sec, 46.86 m/sec and 36.11 m/sec respectively. Thus, the true air velocity is 157.9 m/sec which is well converged to the flight speed at M = 0.5 and h = 6096 m.

*Figure 3* shows the responses of roll rate ($p/\Delta\delta_{ar}$), pitch rate ($q/\Delta\delta_{et}$) and yaw rate ($r/\Delta\delta_{ar}$). The steady-state amplitudes of the roll, pitch and yaw rates are equal to $7.326\times10^{-5}$ rad/sec, $4.26\times10^{-5}$ rad/sec and $-8.486\times10^{-4}$ rad/sec respectively. *Figure 4* shows the responses of the bank "roll" angle ($\Phi/\Delta\delta_{ar}$), pitch angle ($\theta/\Delta\delta_{et}$) and sideslip angle ($\beta/\Delta\delta_{ar}$). The steady-state amplitudes of ($\Phi/\Delta\delta_{ar}$), ($\theta/\Delta\delta_{et}$) and ($\beta/\Delta\delta_{ar}$) equal to -0.05605°, 0.01016° and 0.0742° respectively. Overall, small attitudes and rates were obtained indicating negligible steady-state errors achieved for cruise trim flight. The settling time of two sec was obtained with no obvious attitude overshoots and with peak rates revealing the high levels of perturbations that might be instantaneously experienced. And the $H_\infty$SAD did well to quickly deny them in less than 1.4 sec.

### 4.3 6DOF flight control efforts

As seen in the previous section stably convergent 6DOF flight was achieved under unit step $\Delta\delta_{et}$ of 1° from one hand and unit step $\Delta\delta_{ar}$ of 1° from another hand. The reference input full-state feedback autopilot designs [21] were then combined into the 6DOF B747-100 flight that was already controlled with the $H_\infty$SAD to meet a resultant velocity of 157.9 m/sec and altitude of 6096 m at the same time with

no roll, pitch and yaw effects may be observed. The denominator TF coefficients are based on $\Delta\delta_{ar}$ and $\Delta\delta_{et}$ controls are shown in *Table 2*. The numerator TF coefficients are based on $\Delta\delta_{ar}$ and $\Delta\delta_{et}$ controls are shown in *Table 3*. The characteristic equations are of the 5$^{th}$ order in *s* Laplace variable for each control input.

*Figure 5* shows the control efforts for B747-100 longitudinal trim dynamics when the elevator and throttle are activated. Elevator reached a steady deflection of 0.31 rad (17.76°) in about 20 sec whereas the throttle was actuated to reach 0.58 rad (33.2°) in about 50 sec. It seemed that the throttle doubled its action by increasing the thrust and augmenting the heading speed. However, the elevator is just excited to perform additional 3.44°.
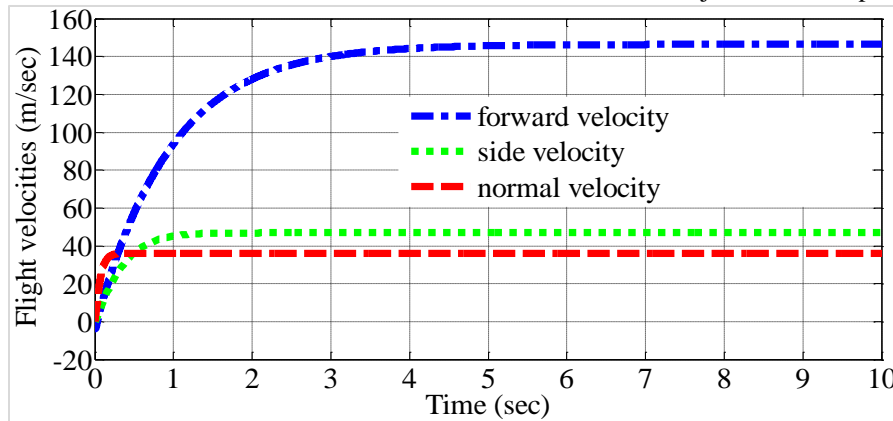


**Figure 2** Forward, side and normal velocities of B747-100 6DOF controlled flight
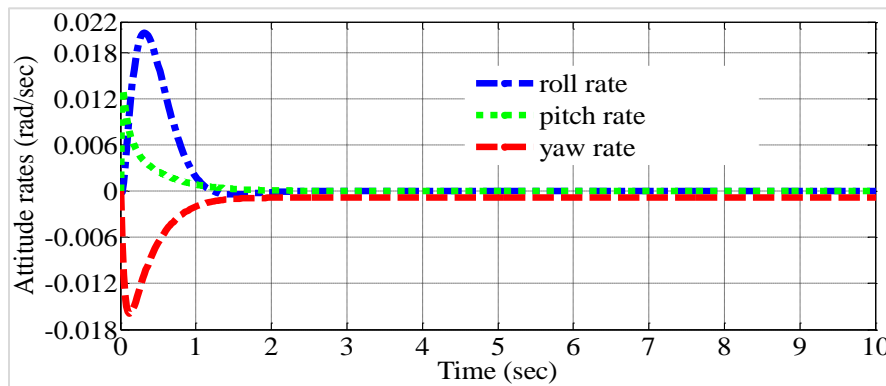


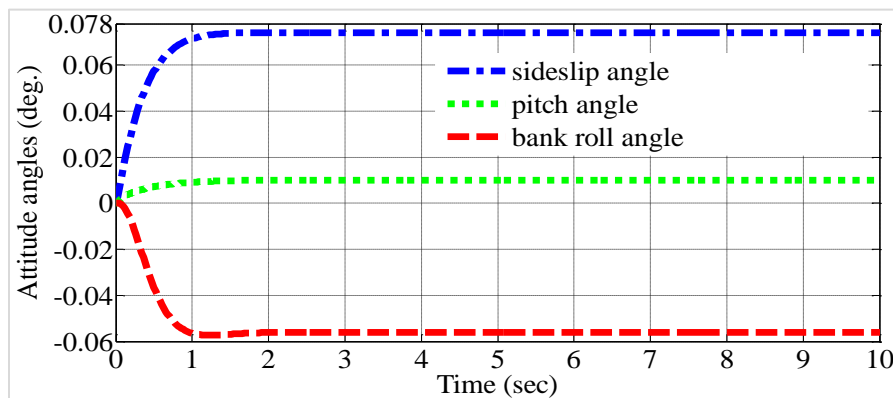**Figure 3** Attitude rates of B747-100 6DOF controlled flight



**Figure 4** Attitude angles of B747-100 6DOF controlled flight

*Figure 6* shows the control efforts for B747-100 lateral trim dynamics when the rudder and aileron are activated. Rudder touched steady-state deflection of 0.408 rad (23.38°) in about 64.3 sec whereas aileron reached 0.234 rad (18.68°) of steady deflection in about 26.9 sec. As expected, the rudder as a vertical control surface acquired longer to settle down compared with the aileron horizontal control surface.

**Table 2** Denominator transfer function based on $\Delta\delta_{et}$ and $\Delta\delta_{ar}$ controls of 6DOF B747-100 flight

| I | S | $b_0$ | $b_1$ | $b_2$ | $b_3$ | $b_4$ | $b_5$ |
|---|---|---|---|---|---|---|---|
| $\Delta\delta_{et}$ | u w q θ h α | 0.75 | 7.513 | 25.62 | 43.79 | 15.9 | 1.98 |
| $\Delta\delta_{ar}$ | v p r Φ β | 7.31 | 25.79 | 22.81 | 6.42 | 1.0 | 0 |

I and S stand for control inputs and flight state characteristics respectively. The remaining variables are already defined in the previous sections.

**Table 3** Numerator transfer function based on $\Delta\delta_{et}$ and $\Delta\delta_{ar}$ controls of 6DOF B747-100 flight

| I | S | $a_0$ | $a_1$ | $a_2$ | $a_3$ | $a_4$ |
|---|---|---|---|---|---|---|
| $\Delta\delta_{et}$ | u | 1168.5 | 47.02 | -391 | 5.16 | 0.07 |
| | w | 85.21 | 1623.9 | 29.08 | 6.212 | 0.05 |
| | q | 0 | -0.002 | -3.55 | -0.53 | 0 |
| | θ | 0.180 | 35.51 | 5.32 | 0.005 | 0 |
| | h | 110753 | 210511 | -38613 | -451 | 0 |
| | α | 0.54 | 102.8 | 0.184 | 0.04 | 0 |
| $\Delta\delta_{ar}$ | v | 94.48 | 38.72 | 6.475 | 0.177 | 0 |
| | p | 0 | 0.309 | 0.131 | 0.015 | 0 |
| | r | -0.021 | -0.602 | -0.23 | -0.03 | 0 |
| | Φ | 0.309 | 0.132 | 0.016 | 0 | 0 |
| | β | 0.594 | 0.245 | 0.041 | 0.001 | 0 |

I and S stand for control inputs and flight state characteristics respectively. The remaining variables are already defined in the previous sections.
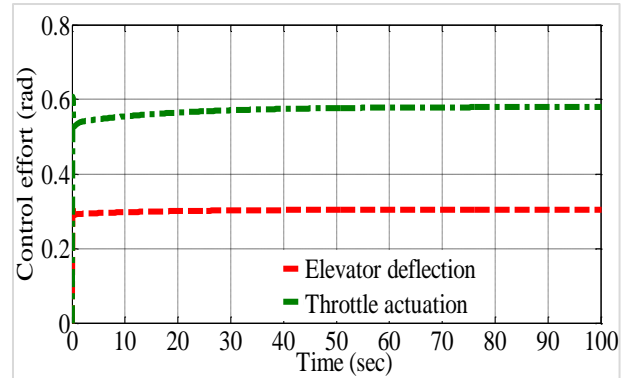


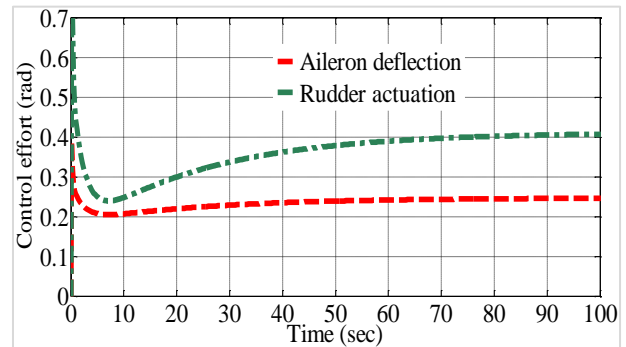**Figure 5** B747-100 longitudinal trim control efforts



**Figure 6** B747-100 lateral trim control efforts

## 4.46DOF flight control validations

The eigenvalue spectrum provides several dynamic stability flight modes and confirms the fulfilment of flying quality properties or the so-called Cooper-Harper scale [8]. The federal aviation regulations (FARs) and/or military specifications (MIL-SPEC) generally regulate a flying level, response period (T) and/or $\omega$ and $\xi$ for stability requirements. Permissible requirements are shown in *Table 4* for the level I mission flight phase [1]. *Table 4* also shows 6DOF flight modes (PH, SP, SC, RS and DR) identified at the baseline condition of M = 0.5 and h = 6096 m. The DR mode was satisfied as natural frequency, damping ratio and their product were being met those merits. Also, the SC and RS response periods well obey those merits.

**Table 4** B747-100 6DOF flight modes at baseline condition

| Modes of flight (MD) | EV | $\xi$ | $\omega$ | $\xi\omega$ | T | Merits [1] |
|---|---|---|---|---|---|---|
| PH | -0.3±0.26i | 0.69 | 0.36 | 0.25 | 2.83 | $0.04 < \xi$ |
| SP | -3.7±1.87i | 0.89 | 4.1 | 3.65 | 0.244 | $0.7 < \xi < 1.3$ |
| SC | -0.49 | 1 | 0.43 | 0.43 | 2.35 | fairly slow |

| MD | EV | | | | | |
|----|-----------|------|------|------|------|-----------------------|
| **RS** | -1.18 | 1 | 1.18 | 1.18 | 0.85 | 0.33<T<1.4 |
| **DR** | -2.4±2.97i | 0.63 | 3.82 | 2.41 | 0.26 | 0.08< ξ <0.7<br>0.08<ω<br>0.08< ξω |

MD and EV stand for modes of flight and eigenvalues characteristic of stability respectively. The remaining variables are already defined in the previous sections. T, $\omega$ and $\xi\omega$ have the units of sec, rad/sec and rad/sec respectively.

Short period mode contours are widely used to validate the flying qualities where the damping ratio is shown on a log scale because of oval contours prolonged alongside the horizontal axis [1, 8]. Obviously, the pair of natural frequency and damping ratio from the SP mode based on the current work lies inside an acceptable contour and is very close to a satisfactory boundary as shown in *Figure 7*. The short period mode of longitudinal flight with the LQR control showed the eigenvalue of -4.174 ± 2.587i (damping ratio = 0.85 and frequency = 4.91 rad/sec) [10]. It has been also shown the uncontrolled case sat just outside the acceptable boundary at the eigenvalue of -0.9718 ± 2.0404i (damping ratio = 0.43 and frequency = 2.26 rad/sec). Poor handling quality was also found with low longitudinal stability

for uncontrolled flight [18]. The $H_\infty$SAD enhances the Eigenvalue location by pushing it farther on the left-hand side of the $s$ plane. It found at -3.8950 ± 1.2802i (damping ratio = 0.43 and frequency = 2.26 rad/sec) compared with the traditional LQR applied to compensate the longitudinal maneuver alone. It seems that the pitch rate ABC optimization augmented the SP damping ratio compared to [10] which well agrees with [45]. The so-called "Cstar" flying quality criteria [1, 8] would not be assessed as B747-100 old aircraft does not include the sophisticated aerodynamic design or higher-order systems account for advanced criteria. Instead, CAP [45] and pitch-rate flying quality [45] metrics will be evaluated next.
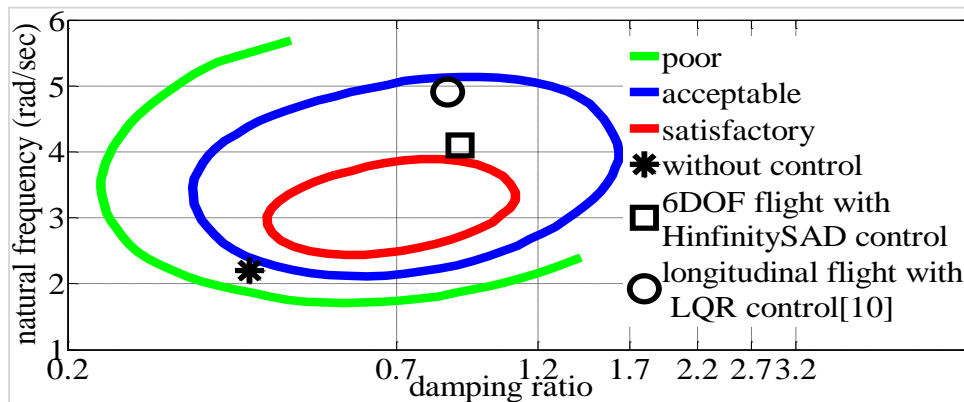


**Figure 7** Flying quality short period mode contours

A range of flight conditions (M from 0.2 to 0.9 and h from sea level to 12190 m) is also checked as shown in *Figure 8* for the stability convergences based on the $H_\infty$SAD and ABC scheme. They showed a comparison with CAP flying qualities criteria on the log-log plot [45]. The CAP indicates the level of quality coincidence between trim flight and pilot [1, 8, 45]. The CAP boundary (the straight-line slope of 0.5) designates SP frequency control measure where large and small CAP describes aircraft as being highly sensitive to abruption and would have sluggish and/or overshooting behaviour respectively. Load factor ratio ($az_\alpha$) was defined by normal load factor to the
728

angle of attack [8] and was computed $az_\alpha = s\,w/\alpha\, -u_0\,q/\alpha$ which was readily found in *Figure 2* and *Figure 3* along with the definition of $\alpha$ being already given in Subsection 3.1. Wide flight cases examined obey CAP criteria and no condition passed the flying quality boundary. And being noted, as M and h are getting low the aircraft is more susceptible to external disturbances and as M and h are getting high the aircraft is at risk of sluggishness and/or overshooting experience. Clearly, the good responses which are already obtained using the $H_\infty$SAD and ABC at M = 0.5 and h = 6096 m (the baseline case) are confirmed in *Figure 8* (see the star symbol) as its CAP measure

indicates a moderately expected flight scenario (neither high abruption/overshot). Such finding is in fair agreement with Murrieta-Mendoza et al. [44]

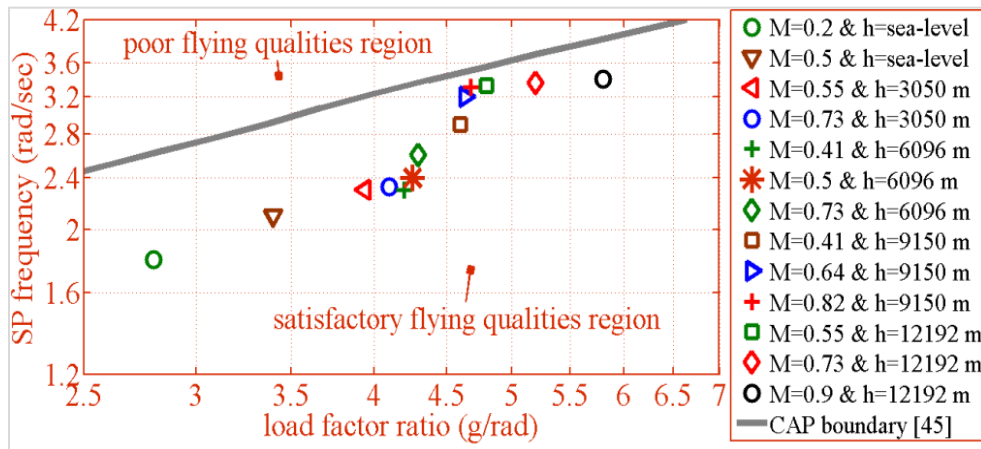who also used the ABC optimisation to show free-flight fulfilling the necessary time of arrival limitation.



**Figure 8** CAP flying qualities for 6DOF B747-100 based on H∞SAD and ABC

The pitch rate criterion was also assessed as shown in *Figure 9* where the steady-state pitch rate was $q/\Delta\delta = 33.92H + 4.62\times10^5 M + 17.26\ HM - 1.08\times10^6/-230.51H - 2.23\times10^6\ M - 109.48\ HM + 8.47\times10^6$ given that its estimated values over the flight envelope vary from $-82.4\times10^{-3}$ to $-143\times10^{-3}$ sec$^{-1}$.

As clearly seen, simulations of various flight conditions well converged inside the pitch-rate boundaries [45] (the grey dashed lines) based on the normalized pitch rate to its steady-state values. The close-up view of the steady-state region also verifies that no divergences are appearing outside the boundaries. All the normalized rates settled to almost levelled responses with slight steady-state errors concerning unit step reference (about -2% to 4% in the most responses) which satisfy the longitudinal trimmed merits of straight, levelled flight. Only some responses of M > 0.73 and h >

6096 m slightly overstepped the boundaries nearby the transient region which is not expected to degrade the flight qualities as occurred in less than 1 sec. This confirms the aircraft is well augmented by the H∞SAD and ABC since B747-100 is expected to have a very slow response (large transient time) due to the inertia effect of its heavy design. The normal acceleration feedback seen in the computation of load factor in *Figure 8* caused augmentation in natural frequency giving high manoeuvrability of the aircraft in coinciding with [1, 8, 45].
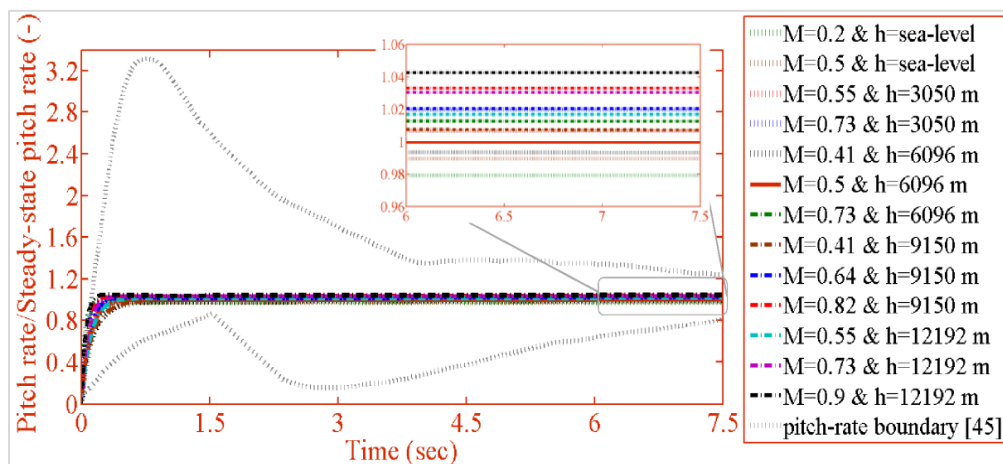


**Figure 9** Pitch rate flying qualities for 6DOF B747-100 based on H∞SAD and ABC

## 5.Discussion

### 5.16Comparative analysis

The qualitative results of converged state variables of the 6DOF simulation of the B747-100 flight were already expected due to the robust reputation of $H_\infty$ controller design law. Most results presented in Section 4 were superbly compensated for the erroneous responses including the unexpected disturbances. The dynamic stabilities were efficiently augmented throughout longitudinal and lateral states shown analytically and confirmed through sets of simulations. It should be emphasized that these state responses were obtained based on the resultant lateral-directional coupling control $\Delta\delta_{ar} = \Delta\delta_a \cup \Delta\delta_r$ and the resultant longitudinal coupling control $\Delta\delta_{et} = \Delta\delta_e \cup \Delta\delta_t$ that was already shown in *Figure 6* and *Figure 5* respectively.

The successful implementation of the ABC algorithm depends on the choice of the initially employed bee matrices $\Omega_{ij}$ and $\Omega_{kj}$ based on the implementation of Equation 17 then Equation 20. The rule of thumbs and/or the trial-and-error procedure performs a major factor in the selection of diagonal patterns. The maximum number of generations was fixed to 1000 and the search space was imposed as $13 \times 18 \times 1000 : 9 \times 9 \times 1000 : 4 \times 9 \times 1000$ which reflects the design spaces matrices dimensions of A: B: C: K etc.

Specifically, the coefficient settings, colony dimension and total cycles of the ABC optimisation procedure were implemented between 0.1 and 100, 15 and 100 respectively. However, the colony size and max cycle may be manipulated in the case of constricted parameter settings to save the computational budget. The algorithm was run for 20 runtimes on each benchmark case before validating the obtained solution.

To further authenticate how great the synthesis of $H_\infty$SAD and ABC algorithms is performing for the model and simulation 6DOF handling of B747-100 flight. *Figure 10* demonstrates the altitude convergences for the landing approach flying scenario of M = 0.2 at sea level and the altitude limit flying scenario of M = 0.9 at 12192 m. As clearly shown, the baseline cruise flight case of M = 0.5 at 6096 m that was being modelled converged well to the flight altitude of $0.609 \times 10000$ m = 6090 m (the simulation error is less than 0.1%). The encryption of $H_\infty$ and ABC algorithms together at a single model and simulation platform was also assured for the altitude convergences at M = 0.2 at sea level and M = 0.9 at 12192 m with less than one per cent of the simulation errors regarding the trim values of 0 and 12192 m respectively.
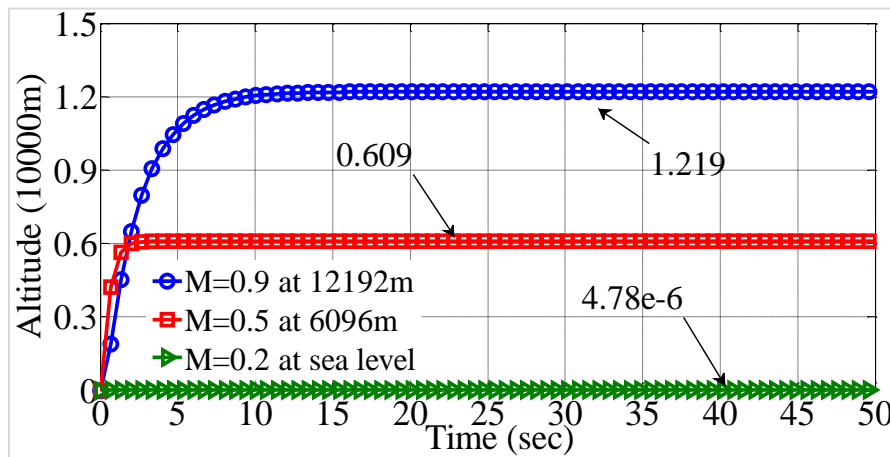


**Figure 10** Validation of altitude convergences in three flight cases

### 5.2Limitations

The accuracy of the $H_\infty$SAD and ABC approach was statistically indicated by using root mean square error and main absolute error metrics. Those standards give the accuracy achieved between measured and predicted values [25−27]. The precision of the ABC optimiser in the estimations of the $H_\infty$SAD weighting

matrices give as high as 90% in regression over the most flight responses achieved. *Table 5* summarises the ABC's parameter settings which are helpful to minimise the cost function $(f_i, i = 1:3)$ in Equation 13 and thus obtain the optimal weighting matrices. *Table 6* statistically compares those objective functions of the ABC procedure. The standard deviation, best, averaged and worst results are

compared with TETR (without systematic optimisation) [10]. Clearly, the ABC algorithm delivers much better convergence stability than without systematic optimisation. At each state variable, the flight response was found to have reasonable features based on the ABC constraints tabulated below. For example, $u$ response of satisfactorily longitudinal flight $H_\infty$SAD-based augmentation has to obey the ABC algorithm constraints of $O_1 < 5\%$ for desired overshoot,

$O_2 \leq 10\%$ for acceptable settling time and $O_3 < \pm 2\%$ of the desired value of Steady State Error (SSE). Fitness control parameter residuals of $F_1 = 0.5$, $F_2 = 0.7$ and $F_3 = 0.9$ have to be deployed to achieve reasonably optimised $H_\infty$ design matrices to augment $u$ response of longitudinal flight. Such demonstration is relevant to the remainder of the state variables tabulated in *Table 5*.

**Table 5** the ABC's parameter settings and limitations

| S | Constraints | | | Fitness | | |
|---|---|---|---|---|---|---|
| | $O_1$ <... (%) | $O_2$ ≤... (sec) | $O_3$ <±... (%) ×**SSE** | $F_1$ | $F_2$ | $F_3$ |
| $u$ | 5 | 10 | 2 | 0.5 | 0.7 | 0.9 |
| $w$ | 3 | 4 | 1.8 | 0.8 | 0.9 | 0.5 |
| $q$ | 3 | 4 | 1.8 | 0.8 | 0.8 | 0.6 |
| $\theta$ | 3 | 5 | 1.7 | 0.7 | 0.9 | 0.5 |
| $h$ | 4 | 10 | 2 | 0.5 | 0.7 | 0.9 |
| $\alpha$ | 2 | 7 | 2 | 0.9 | 0.7 | 0.5 |
| $v$ | 5 | 7 | 2 | 0.5 | 0.7 | 0.9 |
| $p$ | 3 | 4 | 1.6 | 0.5 | 0.7 | 0.95 |
| $r$ | 3 | 4 | 1.7 | 0.5 | 0.7 | 0.9 |
| $\Phi$ | 5 | 5 | 1.9 | 0.9 | 0.5 | 0.7 |
| $\beta$ | 5 | 6 | 2 | 0.7 | 0.8 | 0.6 |

S and SSE stand for flight state characteristics and Steady State Error respectively. The remaining variables are as already defined in the 4.1 subsections.

**Table 6** Accuracy comparison of the ABC cost functions

| Cost function | Optimiser | Worst solution | Best solution | Averaged solution | Standard deviation |
|---|---|---|---|---|---|
| $f_1$ | TETR [10] | 1.18E-02 | 1.24E-3 | 1.73E-02 | 1.43E-02 |
| | ABC | 1.35E-04 | 1.86E-6 | 1.49E-05 | 1.15E-05 |
| $f_2$ | TETR [10] | 3.76E-02 | 4.47E-3 | 1.07E-2 | 2.48E-2 |
| | ABC | 2.04E-03 | 3.81E-5 | 4.55E-4 | 9.02E-3 |
| $f_3$ | TETR [10] | 1.93E-02 | 2.57E-3 | 4.62E-3 | 2.48E-2 |
| | ABC | 0.05E-03 | 9.27E-6 | 6.81E-4 | 1.90E-4 |

Overall, the 6DOF model and simulation of B747-100 aircraft work fine from the mathematical perspective with the linearization consideration around the operating trim conditions for both the longitudinal and lateral flight envelope. Although the simulation is being conducted on the most severe scenario of flight, i.e., the baseline at M = 0.5 and h = 6096 m, the synthesis of $H_\infty$SAD and ABC framework is qualitatively validated for the flying handling quality criteria based on the short period mode contours graph [8]. In the previous study [10], the LQRFSF has shown reasonable responses for a range of databases of M and h sets. However, the

results obtained based on the match of $H_\infty$SAD and ABC strategy are much better than that in [10]. As already being shown in *Figure 7* that the square legend of the present work based on the fusion structure of $H_\infty$SAD and ABC framework is in the vicinity to the satisfactory contours of SP mode longitudinal 6DOF model compared to the LQR counterpart for a decoupled model of longitudinal flight and the scenario of without control flight. This indicates the strategy has been doing well if the ABC optimiser process is deployed for the finest design matrices in terms of how much the overshot per cent allowances, settling intervals and the steady-state

errors and/or the initial perturbation to assure the dynamic stability of aircraft system. However, these stability requirements bind the overall convergence and computation effort. The authors recommend starting with the most achievable criteria and then progressively adding one-by-one merit till the whole design assets are achieved. A complete list of abbreviations is shown in *Appendix I.*

## 6.Conclusion and future work

More freedom is admitted in guaranteeing the output feedback control quadratic performance during the 6DOF B747-100 flight at the baseline case of Mach number of 0.5 and altitude of 6096 m. A quasilinear model has been derived from the decomposition of longitudinal states, elevator and throttle couplings and the lateral-directional states, aileron and rudder couplings. The $H_\infty$SAD tasks are a solvable numerical problem combining the ABC algorithm to feasibly select weighting matrices instead of trivial trial and error methods.

The ABC has shown a deferential optimization capability to accomplish widespread time-based responses comprising settling temporal requiems, overshoot peak responses and erroneous steady states. The designed control regime implements limited feedback information of desired responses. And it is believed that the procedure is flexible enough to take account of other B747-100 flight conditions. The control strategy retains enough effectiveness to ensure a safe recovery to normal flight. The examined eigenvalue spectra well refer to a range of dynamic, stable longitudinal and lateral modes which confirm flying quality fulfilment or even the so-called Cooper-Harper scale for the flight case studied here. The C-star criterion may not be an adequate competency with civil transport aircraft for the analysis of flying and handling qualities since the B747-100 is inherently heavy and well-behaved with minimal augmentation needed.

Finally, the short-period characteristics obtained from 6DOF controlled with the $H_\infty$SAD lay close to a satisfactory boundary of flying quality contours compared with the past work based on a longitudinal flight with LQR control. Other flight modes (PH, DR, SC and RS) also well meet the most flying qualities' merits. Also, verifications for various flight conditions show good respect to CAP and pitch rate flying qualities. The C-star metric is not approached as the B747-100 model does not incorporate advanced aerodynamic high-order functions.

The $\mu$ method analysis might be used to investigate the controller robustness of the 6DOF aircraft model to handle nonlinearities and parametric uncertainties for successfully scheduling different altitudes and Mach numbers. Also, the flying qualities need to be verified for an aero-elasticity model throughout the whole flight envelope using the so-called GS design.

## Conflicts of interest
The authors have no conflicts of interest to declare.

## Author's contribution statement
**Ezzeddin M. Elarbi:** Conceptualization, investigation on challenges, data analysis, data acquisition and writing-original draft. **Abdulhamid A. Ghmmam:** Interpretation of results, review, supervision, reading-proof and the revision of the whole article.

## References
[1] Mclean D. Automatic flight control systems. Measurement and Control. 2003; 36(6):172-5.
[2] Blight JD, Gangsaas D, Richardson TM. Control law synthesis for an airplane with relaxed static stability. Journal of Guidance, Control, and Dynamics. 1986 ; 9(5):546-54.
[3] Shiau JK, Ma DM. An autopilot design for the longitudinal dynamics of a low-speed experimental uav using two-time-scale cascade decomposition. Transactions of the Canadian Society for Mechanical Engineering. 2009; 33(3):501-21.
[4] Shinners SM. Modern control system theory and design. John Wiley & Sons; 1998.
[5] Filasova A, Krokavec D. Control of linear systems using dynamic output controllers. In CS & IT conference proceedings 2014. CS & IT Conference Proceedings.
[6] Xue Y, Jiang J, Zhao B, Ma T. A self-adaptive artificial bee colony algorithm based on global best for global optimization. Soft Computing. 2018; 22(9):2935-52.
[7] Gao H, Shi Y, Pun CM, Kwong S. An improved artificial bee colony algorithm with its application. IEEE Transactions on Industrial Informatics. 2018; 15(4):1853-65.
[8] Howard RM. Dynamics of flight: stability and control. Journal of Guidance, Control, and Dynamics. 1997; 20(4):839-40.
[9] Labit DP, Taitz K. User's Guide for SEDUMI INTERFACE 1.04.
[10] Elarbi EM, Laila DS, Ghmmam AA, Horri N. LQR reference tracking control of Boeing 747-100 longitudinal dynamics with CG shifts. In international

conference on advanced technology & sciences 2017 (pp. 114-24).

[11] Tosun DC, Işık Y, Korul H. LQR control of a quadrotor helicopter. New Developments in Pure and Applied Mathematics. 2015.

[12] Joukhadar A, Hasan I, Alsabbagh A, Alkouzbary M. Integral Lqr-based 6dof autonomous quadrocopter balancing system control. International Journal of Advanced Research in Artificial Intelligence. 2015; 4(5):10-17.

[13] Adir VG, Stoica AM. Integral LQR control of a star-shaped octorotor. Incas Bulletin. 2012; 4(2):3-18.

[14] Bharathi M, Kumar G. An LQR controller design approach for pitch axis stabilisation of 3-DOF helicopter system. International Journal of Scientific & Engineering Research. 2013; 4(4).

[15] Öner KT, Çetinsoy E, Sırımoğlu E, Hancer C, Ayken T, Ünel M. LQR and SMC stabilization of a new unmanned aerial vehicle. International conference on intelligent control, robotics, and automation. 2009 (pp. 58-94).

[16] Sharma V, Voulgaris PG, Frazzoli E. Aircraft autopilot analysis and envelope protection for operation under icing conditions. Journal of Guidance, Control, and Dynamics. 2004; 27(3):454-65.

[17] Lungu R, Lungu M. Automatic landing control using H-inf control and dynamic inversion. Proceedings of the Institution of Mechanical Engineers, Part G: Journal of Aerospace Engineering. 2014; 228(14):2612-26.

[18] Portapas V, Cooke A. Simulated pilot-in-the-loop testing of handling qualities of the flexible wing aircraft. Aviation. 2020; 24(1):1-9.

[19] Rigatos G, Siano P. A new nonlinear H-infinity feedback control approach to the problem of autonomous robot navigation. Intelligent Industrial Systems. 2015; 1(3):179-86.

[20] Zhang H, Liu J, Xu S. H-infinity load frequency control of networked power systems via an event-triggered scheme. IEEE Transactions on Industrial Electronics. 2019; 67(8):7104-13.

[21] Luo W, Chu YC, Ling KV. H-infinity inverse optimal attitude-tracking control of rigid spacecraft. Journal of Guidance, Control, and Dynamics. 2005; 28(3):481-94.

[22] Li SE, Gao F, Li K, Wang LY, You K, Cao D. Robust longitudinal control of multi-vehicle systems—a distributed H-infinity method. IEEE Transactions on Intelligent Transportation Systems. 2017; 19(9):2779-88.

[23] Liu C, Jiang B, Zhang K. Adaptive fault-tolerant H-infinity output feedback control for Lead–Wing close formation flight. IEEE Transactions on Systems, Man, and Cybernetics: Systems. 2018; 50(8):2804-14.

[24] Azar AT, Serrano FE, Koubaa A, Kamal NA. Backstepping h-infinity control of unmanned aerial vehicles with time varying disturbances. In first international conference of smart systems and emerging technologies 2020 (pp. 243-8). IEEE.

[25] Karaboga D, Basturk B. On the performance of artificial bee colony (ABC) algorithm. Applied Soft Computing. 2008; 8(1):687-97.

[26] Baris AT, Coban R. Artificial bee colony algorithm based linear quadratic optimal controller design for a nonlinear inverted pendulum. International Journal of Intelligent Systems and Applications in Engineering. 2015; 3(1):1-6.

[27] Karaboga D, Akay B. A comparative study of artificial bee colony algorithm. Applied Mathematics and Computation. 2009; 214(1):108-32.

[28] Richardson TS, Beaverstock C, Isikveren A, Meheri A, Badcock K, Da RA. Analysis of the Boeing 747-100 using CEASIOM. Progress in Aerospace Sciences. 2011; 47(8):660-73.

[29] Yu B, Zhang Y. Fault-tolerant control of a boeing 747-100/200 based on a laguerre function-based mpc scheme. IFAC-PapersOnLine. 2016; 49(17):58-63.

[30] Hameed AS, Bindu GR. Gain scheduled finite horizon LQR for approach and landing phase of a reusable launch vehicle. Journal of The Institution of Engineers (India): Series C. 2022; 103:381-8.

[31] Eser S, Çetin ST. Optimum control of a flexible single link manipulator with artificial bee colony algorithm. Proceedings of the Institution of Mechanical Engineers, Part C: Journal of Mechanical Engineering Science. 2022; 236(7):3731-42.

[32] Ma R, Wu H, Ding L. Artificial bee colony optimised controller for small-scale unmanned helicopter. The Aeronautical Journal. 2017; 121(1246):1879-96.

[33] Saied M, Slim M, Mazeh H, Francis C, Shraim H. Unmanned aerial vehicles fleet control via artificial bee colony algorithm. In 4th conference on control and fault tolerant systems 2019 (pp. 80-5). IEEE.

[34] Du H, Liu P, Cui Q, Ma X, Wang H. PID controller parameter optimized by reformative artificial bee colony algorithm. Journal of Mathematics. 2022.

[35] Cai X, Liu H. A six-degree-of-freedom proportional-derivative control strategy for bumblebee flight stabilization. Journal of Biomechanical Science and Engineering. 2021; 16(4):1-23.

[36] Du H, Cui Q, Liu P, Ma X, Wang H. Reformative artificial bee colony algorithm based PID controller for radar servo system. Electronic Research Archive. 2022; 30(8):2941-63.

[37] Sheida K, Nobari M, Baigzadehnoe B, Bevrani H. An artificial bee colony based PID controller for depth control of an autonomous underwater vehicle. In 8th international conference on control, instrumentation and automation 2022 (pp. 1-6). IEEE.

[38] Jouda MS, Kahraman N. Improved optimal control of transient power sharing in microgrid using h-infinity controller with artificial bee colony algorithm. Energies. 2022; 15(3):1-26.

[39] Bijani V, Khosravi A. Robust PID controller design based on H∞ theory and a novel constrained artificial bee colony algorithm. Transactions of the Institute of Measurement and Control. 2018; 40(1):202-9.

[40] Bansal JC, Gopal A, Nagar AK. Stability analysis of artificial bee colony optimization algorithm. Swarm and Evolutionary Computation. 2018; 41:9-19.

[41] Sharma TK, Abraham A. Artificial bee colony with enhanced food locations for solving mechanical engineering design problems. Journal of Ambient Intelligence and Humanized Computing. 2020; 11(1):267-90.

[42] Zhou G, Moayedi H, Bahiraei M, Lyu Z. Employing artificial bee colony and particle swarm techniques for optimizing a neural network in prediction of heating and cooling loads of residential buildings. Journal of Cleaner Production. 2020.

[43] Jarrah MI, Jaya AS, Alqattan ZN, Azam MA, Abdullah R, Jarrah H, et al. A novel explanatory hybrid artificial bee colony algorithm for numerical function optimization. The Journal of Supercomputing. 2020; 76(12):9330-54.

[44] Murrieta-mendoza A, Botez RM, Bunel A. Four-dimensional aircraft en route optimization algorithm using the artificial bee colony. Journal of Aerospace Information Systems. 2018; 15(6):307-34.

[45] Raol JR, Singh J. Flight mechanics modeling and analysis. CRC Press; 2008.

**Ezzeddin M. Elarbi** was born in Tripoli, Libya, in 1976. He received a B.Sc. degree in Aeronautical Engineering from the Tripoli University, Aeronautical Engineering Department, the first-class honour, in 2000. He obtained the Aeronautical Engineering Diploma from the University of Tripoli, the first-class honour, in 2003. He got an M.Sc. degree in control systems from the University of Sheffield, with distinction, in 2006. He obtained a PhD degree from the University of Sheffield, Mechanical Engineering Department. He is the main author of more than 30 conference and journal papers. From 2011 and up to date, he is a lecturer in systems modelling and simulation, numerical methods, and automatic control systems modules. He is now an Associate Professor at the University of Tripoli. He is a supervisor of numerous projects in the field of automatic control systems. His research interests concentrate on optimization, numerical techniques, artificial intelligence control and systems modelling and simulation. Dr Elarbi has been a member of the engineering union since 2001. He has been also a member of the Mathworks community since 2006 and a member of the CFD online society since 2007. He is a member of AIAA and RAeS since 2008.
Email: ezzely5@yahoo.com

**Abdulhamid A. Ghmmam** was born in Tripoli, Libya, in 1959. He received a B.Sc. degree in Aeronautical engineering from the University of Tripoli in 1980. He got his M.Sc. from Canada, Carleton University in 1987 and his PhD from Warsaw University of Technology in 1998. He was the Dean of engineering faculty at the University of Tripoli for over four years. He has teaching experience of 30 years, and he has published many research articles in international journals and conference proceedings. His research area includes Flight Mechanics, Dynamics of Flight and the Aerodynamic Theory.
Email: aaghmam@aerodept.edu.ly

## Appendix I

| S. No. | Abbreviation | Description |
|---|---|---|
| 1 | 6DOF | Six Degree of Freedom |
| 2 | ABC | Artificial Bee Colony |
| 3 | B747 | Boeing® 747 |
| 4 | B747-100/B747-200 | Boing 747-100/200 |
| 5 | CIII | Category III of Flying Quality Criteria |
| 6 | CAIS | Computerised Aircraft Integrated Synthesis |
| 7 | CAP | Control Anticipation Parameter |
| 8 | CTG | Computational Tuning Guidelines |
| 9 | DR | Dutch Roll Oscillatory Mode |
| 10 | FAA | Federal Aviation Administration |
| 11 | FARs | Federal Aviation Regulations |
| 12 | FOC | Feedback Output Control |
| 13 | GS | Gain Scheduling |
| 14 | $H_2$ | H-two Method |
| 15 | $H_\infty$ | H-infinity Method |
| 16 | $H_\infty$SAD | H.Infinity Stability Augmentation Design |
| 17 | IETM | Information Exchange Topology Matrix |
| 18 | JM-FCL | Jacobian Matrices Feedback Control Law |
| 19 | LF | Lyapunov Functions |
| 20 | LFMPC | Laguerre Functions Model Predictive Control Scheme |
| 21 | LQR | Linear Quadratic Regulator |
| 22 | LT-RL | Laplace Transformation and Root Locus method |
| 23 | M | Mach Number |
| 24 | MD | Modes of Flight |
| 25 | MIL-SPEC | Military Specifications |
| 26 | OO | Optimal Observer |
| 27 | PD | Proportional-Derivative |
| 28 | PH | Phugoid or Long Period Mode |
| 29 | PID | Proportional-Integral-Derivative |
| 30 | Qball-X4 | Quadrotor X4 |
| 31 | QSUAVE | Quadrotor Sabanci University Unmanned Aerial Vehicle |
| 32 | RABC | Reformative Artificial Bee Colony |
| 33 | RS | Rolling Subsidence Mode |
| 34 | SC | Spiral Convergence Mode |
| 35 | SSE | Steady State Error |
| 36 | TETR | Trial and Error Thumps Rule |